



## A GENERALIZED CANOPY MODEL FOR THE WIND PREDICTION IN THE FOREST AND THE URBAN AREA

Atsushi Yamaguchi<sup>1</sup>, Kota Enoki<sup>2</sup> and Takeshi Ishihara<sup>3</sup>

<sup>1</sup> Research Associate, Department of Civil Engineering, The University of Tokyo  
7-3-1 Hongo Bunkyo Tokyo 113-8656 Japan [atsushi@bridge.t.u-tokyo.ac.jp](mailto:atsushi@bridge.t.u-tokyo.ac.jp)

<sup>2</sup> Graduate Student, <sup>3</sup> Professor, Department of Civil Engineering, The University of Tokyo

### ABSTRACT

In this study, a generalize canopy model that can consider vegetation, buildings and porous obstacles is proposed. Flow field around two obstacles with different porosities are simulated. The results show a good agreement with the measurement. A wind tunnel test of the scale model of a city is also performed and simulated flow field by proposed mode was verified. The proposed model shows good agreement with the measurement.

**KEYWORDS:** CANOPY MODEL, WIND PREDICTION, URBAN AREA

### Introduction

In order to predict the wind in the urban or dense forest area, canopy models, which consider the effect of the obstacles as external forces, have been proposed. However conventional urban canopy models have the disadvantage of inapplicability to the high packing density canopy. In the prediction of wind in urban area, grids with high packing density are often generated. In this study, a new general canopy model which can consider the effect of the vegetation and solid buildings simultaneously is proposed and verified by wind tunnel test and the onsite measurement.

### Generalized canopy model

#### Governing equations

For the analysis of the flow field with solid inside, two different methods were proposed. In the first approach, the governing equations are constructed for the fluid part only. In the other approach, the governing equations are constructed for the flow field averaged over the computational cell. In this study, the latter approach is used. The account for the effect of the buildings and the vegetation, source and sink terms are added to the non-linear wind prediction model, MASCOT as follows.

$$\frac{\partial \bar{u}_i}{\partial x_i} = 0 \quad (1)$$

$$\frac{\partial \rho \bar{u}_i}{\partial t} + \frac{\partial \rho \bar{u}_j \bar{u}_i}{\partial x_j} = -\frac{\partial \bar{p}}{\partial x_i} + \frac{\partial}{\partial x_j} (\mu \frac{\partial \bar{u}_i}{\partial x_j} - \overline{\rho u'_i u'_j}) + f_{u,i} \quad (2)$$

where  $\bar{u}_i$  and  $u'_i$  are the mean and the fluctuating component of the wind velocity in the  $i$  th direction.  $\bar{p}$  is the pressure,  $\rho$  is the density of the fluid,  $\mu$  is the molecular viscosity  $\overline{\rho u'_i u'_j}$  is the Reynolds stress and  $f_{u,i}$  is the fluid force per unit grid volume on the obstacles which will be described in the next section.

The packing density of a computational grid with the volume of  $V_{\text{grid}}$  in which the volume of  $V_0$  is occupied by an obstacle, can be represented as:

$$\gamma_0 = \frac{V_0}{V_{\text{grid}}} \quad (3)$$

The porosity of a grid  $\gamma_f$  can be written as

$$\gamma_f = 1 - \gamma_0 \quad (4)$$

The relationship between the physical quantity averaged over whole the grid  $\bar{\phi}$  and the quantity averaged over the fluid volume  $\tilde{\phi}$  can be written as

$$\bar{\phi} = \gamma_f \tilde{\phi} = (1 - \gamma_0) \tilde{\phi} \quad (5)$$

The Reynolds stress  $\overline{\rho u'_i u'_j}$  is approximated by the linear turbulence viscosity model.

$$\overline{\rho u'_i u'_j} = \frac{2}{3} \rho k \delta_{ij} - 2\mu_t S_{ij} \quad (6)$$

The turbulence viscosity  $\mu_t$  and  $S_{ij}$  can be written as

$$\mu_t = C_\mu \rho \frac{k^2}{\varepsilon} \quad (7)$$

$$S_{ij} = \frac{1}{2} \left( \frac{\partial \bar{u}_i}{\partial x_j} + \frac{\partial \bar{u}_j}{\partial x_i} \right) \quad (8)$$

The turbulence of flow is estimated by the standard  $k - \varepsilon$  model.

$$\frac{\partial \rho \bar{k}}{\partial t} + \frac{\partial \rho \bar{u}_j \bar{k}}{\partial x_j} = \frac{\partial}{\partial x_j} \left[ \left( \mu + \frac{\mu_t}{\sigma_k} \right) \frac{\partial \bar{k}}{\partial x_j} \right] - \overline{\rho u'_i u'_j} \frac{\partial \bar{u}_i}{\partial x_j} - \rho \bar{\varepsilon} + f_k \quad (9)$$

$$\frac{\partial \rho \bar{\varepsilon}}{\partial t} + \frac{\partial \rho \bar{u}_j \bar{\varepsilon}}{\partial x_j} = \frac{\partial}{\partial x_j} \left[ \left( \mu + \frac{\mu_t}{\sigma_\varepsilon} \right) \frac{\partial \bar{\varepsilon}}{\partial x_j} \right] - C_{\varepsilon 1} \frac{\bar{\varepsilon}}{k} \overline{\rho u'_i u'_j} \frac{\partial \bar{u}_i}{\partial x_j} - C_{\varepsilon 2} \frac{\rho \bar{\varepsilon}^2}{k} + f_\varepsilon \quad (10)$$

In these equations, physical variables are treated as apparent variables. The terms  $f_k$  and  $f_\varepsilon$  is the generation/dissipation of turbulence per unit grid volume within canopy layer described in the next section.

### Generalization of external force

Fluid force on any bluff body is described with the drag coefficient  $C_D$  and a reference area  $A_o$  as,

$$f_{u,i} = -\frac{1}{2} \rho C_D A_o |\bar{u}_i| \bar{u}_i \quad (11)$$

Based on this equation,  $f_{u,i}$  in equation (1) is derived as below.

$$f_{u,i} = \frac{F_{u,i}}{V_{\text{grid}}} = -\frac{1}{2} \rho C_f \frac{1}{l_o} \gamma_o |\bar{u}_i| \bar{u}_i, \quad C_f = \frac{C_D}{(1 - \gamma_o)^2}, \quad l_o = \frac{V_o}{A_o} \quad (12)$$

where  $C_f$  is also a kind of the drag coefficient,  $l_o$  is defined as the representative length scale of obstacles. In case of buildings whose cross section is square,  $l_o$  corresponds to its depth. In this equation, the drag coefficient  $C_f$ , characteristic length  $l_o$  and the packing density  $\gamma_o$  are the physically defined parameters. In the following sections, the relationship between these parameters and the parameters in the conventional models are investigated.

### The modeling of the urban canopy

Maruyama proposed a model to describe the fluid force in urban canopy, in which the fluid force per unit volume can be written as

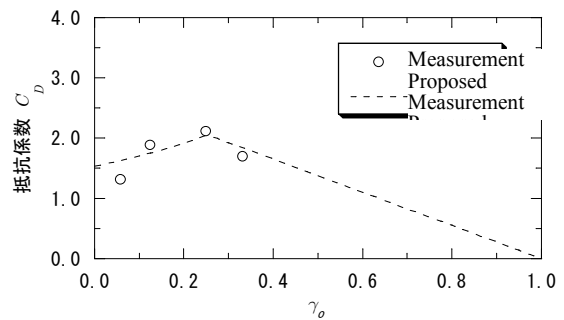


Figure 1. The packing density and the drag coefficient

$$f_{\tilde{u},i} = -\frac{F_{\tilde{u},i}}{V_{\text{fluid}}} = -\frac{1}{2}\rho C_D \frac{A_o}{V_{\text{fluid}}} |\tilde{u}| \tilde{u}_i \quad (13)$$

Maruyama carried out a set of wind tunnel test for building models with different packing density and obtained the drag coefficient  $C_D$ . Figure 1 shows the drag coefficient for different packing density. The white circles in the figure show the results of the wind tunnel test. The drag coefficient  $C_D$  is a function of packing density  $\gamma_o$  and the maximum value is about 3.0, when the packing density is around 20% to 30% and it gradually decreases with increasing of  $\gamma_o$ . Considering those data, the drag coefficient  $C_f$  is modeled like below for urban canopy. Based on these measurements, in this study, a model for the drag coefficient  $C_D$  of urban canopy is proposed.

$$C_D = \min\left(\frac{1.53}{(1-\gamma_o)}, 2.75(1-\gamma_o)\right) \quad (14)$$

In order to prevent numerical instability, the value of  $\gamma_o$  is limited from 0 to  $1-\delta$ .  $\delta$  takes the constant value of  $10^{-4}$ . This additional term does not cause significant change in the flow field.

### The modeling of the vegetation

The fluid force by the vegetation is usually described as

$$f_{\text{tree}} = -\frac{1}{2}\rho\eta C_{D,t} a_t |\bar{u}| \bar{u}_i \quad (15)$$

Where,  $C_{D,t}$  is the drag coefficient of the vegetation,  $a_t$  is the leaf area density and  $\eta$  is the tree crown density and defined as

$$\eta = \frac{V_C}{V_{\text{grid}}} \quad (16)$$

These parameters can be expressed by the parameters in the proposed model and their relationship becomes as follows.

$$C_f = C_{D,t} \quad (17)$$

$$\gamma_o = \frac{V_{\text{leaf}}}{V_{\text{grid}}} = \frac{V_C}{V_{\text{grid}}} \frac{V_{\text{leaf}}}{V_C} = \eta\gamma_{o,c} \quad (18)$$

$$l_o = \frac{V_{\text{leaf}}}{S_{\text{leaf}}} = \frac{\gamma_{o,c} V_C}{S_{\text{leaf}}} = \frac{\gamma_{o,c}}{a_t} \quad (19)$$

### The modeling of the porous media

According to Burk-Plummer, the fluid force in the porous media with the packing density  $\gamma_o$  and the average diameter of the porous sphere  $\bar{D}$  is expressed as

Table 1 The relationship of the parameters for different obstacle models

Type of the obstacles	Fluid force	The relationship of the parameters
Porous media	$f_{u,i} = -\frac{C\rho}{\bar{D}} \frac{\gamma_o}{(1-\gamma_o)^3}  \bar{u}  \bar{u}_i,$ $\bar{D} = C_S V_{\text{porous}} / S_{\text{porous}}$	$C_f = \frac{4C}{3(1-\gamma_o)^3}$ $l_o = 2\bar{D}/3$
Vegetation	$f_{u,i} = -\frac{1}{2}\rho\eta C_{D,t} a_t  \bar{u}  \bar{u}_i$ $\eta = V_C / V_{\text{grid}}$ $a_t = S_{\text{leaf}} / V_C$	$C_f = C_{D,t}$ $l_o = \gamma_{o,c} / a_t$ $\gamma_o = \eta\gamma_{o,c}$
Urban canopy	$f_{u,i} = -\frac{1}{2}\rho C_D a_b  \tilde{u}  \tilde{u}_i$ $a_b = \frac{A_o}{(1-\gamma_o)V_{\text{grid}}}$	$C_f = C_D / (1-\gamma_o)^3$ $l_o = V_o / A_o$ $\gamma_o = V_o / V_{\text{grid}}$

$$f_{u,i} = -\frac{C\rho}{D} \frac{\gamma_o}{(1-\gamma_o)^3} |\bar{u}| \bar{u}_i \quad (20)$$

Where  $C$  is the empirical constant and usually takes the value of 1.75. The characteristic length scale of the porous media can be defined as the ratio of the volume  $V_o$  and the projection area  $A_o$  of the sphere.

$$l_o = \frac{V_o}{A_o} = \frac{\pi \bar{D}^3}{6} \bigg/ \left( \frac{\pi \bar{D}^2}{4} \right) = \frac{2\bar{D}}{3} \quad (21)$$

Equivalent drag coefficient  $C_f$  can be expressed as.

$$C_f = \frac{4C}{3(1-\gamma_o)^3} \quad (22)$$

Table 1 summarises the relationship between the model parameters proposed in this study and the parameters in the conventional models. As a consequent, any external force model can be described by the proposed model. In this sense, this model can be called ‘‘Generalized canopy model’’.

### *The modeling of the source term of turbulent kinetic energy*

For the source terms for turbulent kinetic energy and its dissipation rate, Green’s model that considers the promoting process of energy cascade in canopy layer is adopted.

$$F_k = \beta_p \rho \frac{C_f \gamma_o \bar{\varepsilon}}{2l_o \bar{k}} \sqrt{u_j^2}^3 \left( 1 - \frac{\beta_d}{\beta_p} \frac{\bar{k}}{\sqrt{u_j^2}} \right), f_\varepsilon = C_{pe1} \beta_p \rho \frac{C_f \gamma_o \bar{\varepsilon}}{2l_o \bar{k}} \sqrt{u_j^2}^3 \left( 1 - \frac{C_{pe2} \beta_d}{C_{pe1} \beta_p} \frac{\bar{k}}{\sqrt{u_j^2}} \right) \quad (23)$$

where the model constants  $\beta_p$ ,  $C_{pe1}$ ,  $C_{pe2}$  are set to 1.0, 1.5, 1.0 respectively. Although 4.0 is used for  $\beta_d$ , generally,  $\beta_d$  should be the function of the packing density  $\gamma_o$ . In this study, the generation and dissipation of turbulence in the equation (15) assumed to be canceled out in high packing density region. Then next equation is obtained.

$$\beta_d = \left( \sqrt{u_j^2}^2 / \bar{k} \right) \quad (24)$$

In this study, numerical simulations for high packing density (more than 0.5) are conducted to estimate the relationship between  $\beta_d$  and  $\gamma_o$  under the assumption of the equation (9). At last  $\beta_d$  is modeled like,

$$\beta_d' = C_{m1} \exp\left(\frac{1-\gamma_o}{\gamma_o}\right) + C_{m2} \quad (25)$$

Model parameters are identified and result to be  $C_{m1}=0.489$  and  $C_{m2}=-0.4796$ . Finally model parameter  $\beta_d$  is introduced like

$$\beta_d = \min(4.0, \beta_d') \quad (26)$$

## **Verification of the proposed model**

In order to verify the proposed generalized canopy model, three different flows with different porosities were calculated and compared with the measurement.

### *Flow behind a tree*

The first example is the flow behind a pine tree with 7m height (Figure 2). Kurotani et al. measured the mean and fluctuating wind speed behind the pine tree at the height of  $1.5H$ ,  $3.0H$ ,  $4.5H$  and  $6.0H$ . In this study, as the drag coefficient and leaf area density, 0.8 and  $1.17 \text{ (m}^{-1}\text{)}$  are used respectively, which correspond to  $l_o = 0.0427 \text{ (m)}$  and  $C_f = 0.8$  assuming that the packing density in the crown  $\gamma_{o,c}$  is 0.05. As the inlet boundary condition, wind speed profile is given as in table 1, which is based on the measurement data by Suzuki et al.. The surface roughness length at the ground is set to  $0.0858 \text{ (m)}$ .

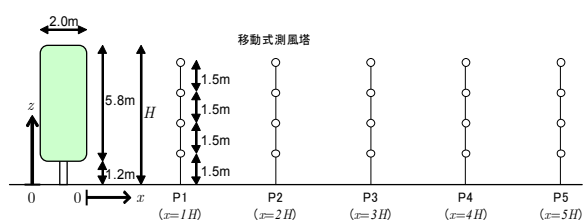


Figure 2 The flow behind a pine tree

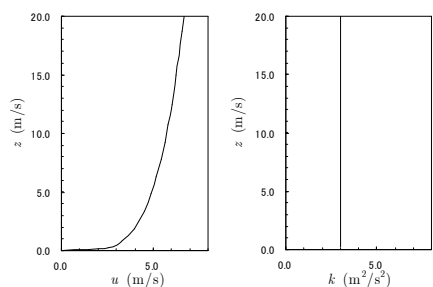


Figure 3 The inflow used for the simulation

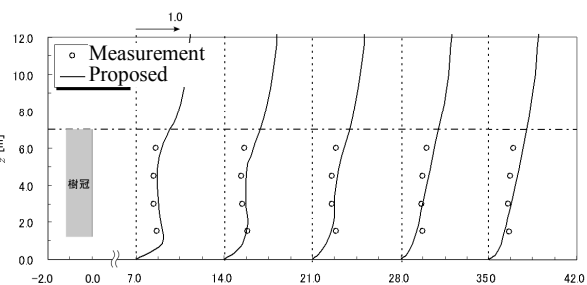


Figure 4. The mean wind speed behind a pine tree

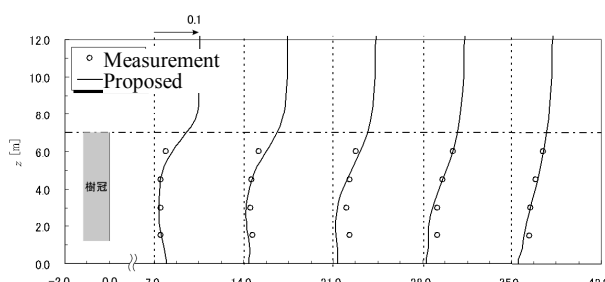


Figure 5. The turbulent kinetic energy behind a pine tree

Figure 4 and 5 shows the vertical profile of the measured and the simulated mean wind speed and turbulent kinetic energy. The dash-dot line shows the height of the tree. The mean wind speed and the turbulent kinetic energy in the figures are normalized by the inflow wind speed (5.3m/s) and its square respectively. The simulated mean wind speed shows a good agreement with the measurement. On the other hand, the turbulent kinetic energy slightly underestimates

### Flow behind a prism

The second example was a flow behind a prism (Figure 6). The aspect ratio of the prism is 1:1:2 and the width is 8cm. The length, width and height of the computational domain is 21.0b, 13.75b and 11.25b respectively. The minimum vertical grid size near the prism is 0.05b and the minimum horizontal grid size is 0.07b (Figure 6). The vertical profile of the mean wind speed and the turbulent kinetic energy at the inlet boundary is shown in figure 7. As the bottom boundary condition, the surface roughness  $z_0 = 1.8 \times 10^{-4}$  (m) was used. At the prism, no surface roughness was set. The simulation results are shown in Figure 4. For the grids which overlap with the prism, the packing density  $\gamma_0$  and the length scale  $l_0$  was calculated and the drag coefficient was calculated.

Figure 8 shows the vertical and horizontal profile of the mean wind energy and the turbulence kinetic energy. The black dashed lines show the reference line along which the wind speed was measured. The simulated wind field shows good agreement with the measurement although slight underestimation of the wind speed in the wake region can be found. The simulated turbulent kinetic energy also shows good agreement with the measurement especially at the front and the side of the prism.

### Flow in urban area

In order to verify the proposed model for the flow around multiple obstacles, the proposed model was verified by a wind tunnel test with an urban model.

The computational domain is 10.3km(x)×7.3km(y)×1.5km(z) and the wind speed was measured at the center of the model. The minimum horizontal grid size is 30m at the center of the model and the minimum vertical grid size is 3.0m at the ground surface, which results in

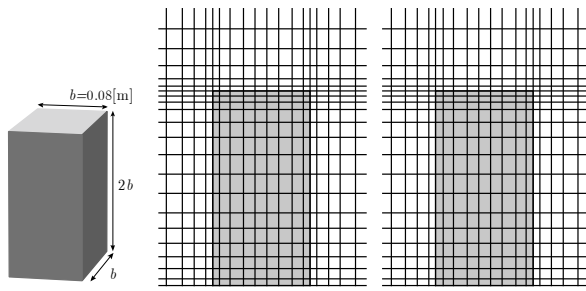


Figure 6 Flow around the prism

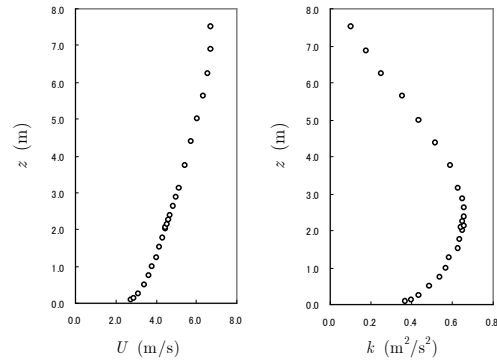


Figure 7 The vertical profile of the inflow

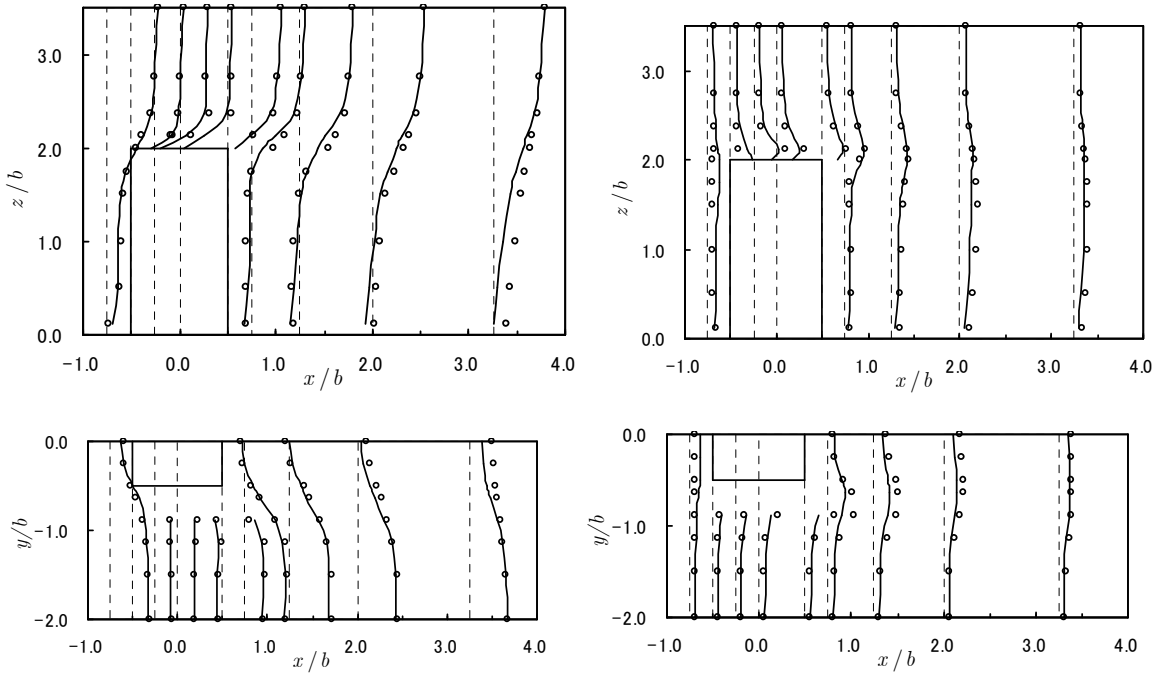


Figure 8 The vertical and the horizontal profile of mean wind speed and turbulent kinetic energy

the total grid number of 194,000. At the inlet boundary, measured vertical profile of the wind speed was given.

The shape, height and the position of the buildings in the city are decided by using a digital map “Zmap-TOWN2” issued by Zenrin Corporation. It contains vector outline and the number of floors of the building. The average floor height is assumed to be 3.5m. Figure 5(a) shows the digital map of the city near the center of the model and (b) shows the calculated plan area for each grid. Perimeter and average building heights are also calculated.

Figure 6 shows the wind speed ratio at the height of 13.5m. In addition to the wind tunnel test and the result of the proposed model is shown. The proposed

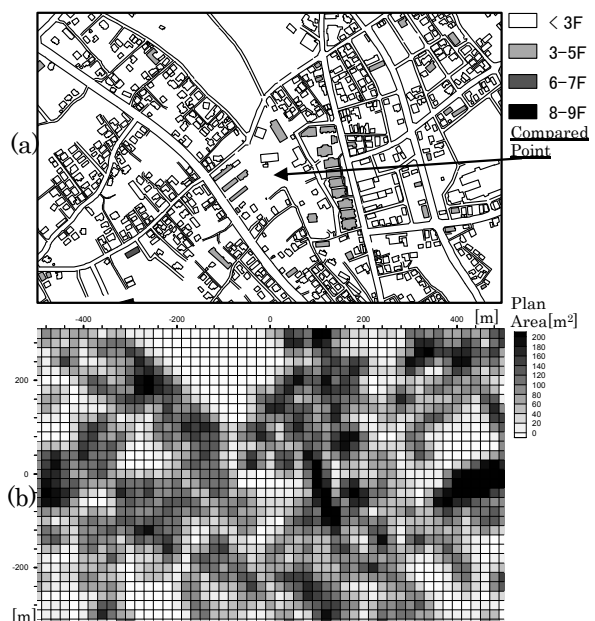


Figure 5 Calculation of model parameters

canopy model shows agreement with the measurement.

### Conclusions

In this study, a generalize canopy model that can consider different kind of obstacles (vegetation, urban canopy and porous obstacles) is proposed. Flow field around two obstacles with different porosities are simulated. The results show good agreements with the measurement. A wind tunnel test of the scale model of a city is also performed and simulated flow field by proposed mode was verified. The proposed model shows good agreement with the measurement.

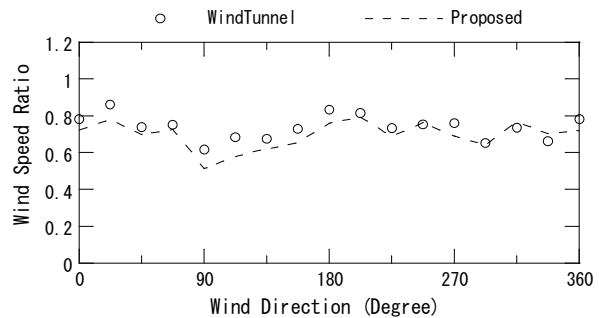


Figure 6 Normalized wind speed at 13.5m

### Reference

- Maruyama, T.: Optimization of roughness parameters for staggered arrayed cubic blocks using experimental data, *J. of Wind Engineering*, No.52, pp.424-429, 1992.
- Burke, S.P, Plummer, W.B., Gas Flow through Packed Columns, *Industrial and engineering chemistry*, vol.20, No.11, p.p.1196-1200, 1928.11.
- Green, S.R., Modeling Turbulent Air Flow in a Stand of Widely Spaced Trees, *PHOENICS Journal Computational Fluid Dynamics and its Applications*, 5, pp.294-312, 1992.
- Kurotani, Y., Kiyota, N., Kobayashi, S., Windbreak effect of Tsuijimatsu in Izumo Part.2, *Proceeding of Annual Meeting Architectural Institute of Japan (D-2)*, pp.745-746, 2001. (In Japanese).
- Ishihara, T., Hibi, K., Measurement of flow and turbulence around the high-rise building, *Journal of Wind Engineering*, Vol.76, pp.55-64, 1998. (In Japanese).
- Ishihara, T., Yamaguchi, A., Takahara, K., Mekar, T., Shinjo, F., Evaluation of maximum wind speed during typhoon 0314 using wind tunnel test and numerical simulation, Architectural Institute of Japan, *Journal of Structural Engineering*, Vol.51A, 2005.3 (In Japanese).